Front. Struct. Civ. Eng. 2016, 10(3): 291–302
DOI 10.1007/s11709-016-0340-3

RESEARCH ARTICLE

Performance assessment of innovative seismic resilient steel knee braced frame

Tony T. Y. YANG[a,b,*], **Yuanjie LI**[b]

[a] *International Joint Research Laboratory of Eearthquake Engineering, 1239 Siping Road, Shanghai 200002, China*

[b] *Department of Civil Engineering, University of British Columbia, Vancouver, BC, V6T 1Z4, Canada*

[*] *Corresponding author. E-mail: yang@civil.ubc.ca*

ABSTRACT Buckling restrained knee braced truss moment frame (BRKBTMF) is a novel and innovative steel structural system that utilizes the advantages of long-span trusses and dedicated structural fuses for seismic applications. Steel trusses are very economical and effective in spanning large distance. However, conventional steel trusses are typically not suitable for seismic application, due to its lack of ductility and poor energy dissipation capacity. BRKBTMF utilizes buckling restrained braces (BRBs) as the designated structural fuses to dissipate the sudden surge of earthquake energy. This allows the BRKBTMF to economically and efficiently create large span structural systems for seismic applications. In this paper, a prototype BRKBTMF office building located in Berkeley, California, USA, was designed using performance-based plastic design procedure. The seismic performance of the prototype building was assessed using the state-of-the-art finite element software, OpenSees. Detailed BRB hysteresis and advanced element removal technique was implemented. The modeling approach allows the simulation for the force-deformation response of the BRB and the force redistribution within the system after the BRBs fracture. The developed finite element model was analyzed using incremental dynamic analysis approach to quantify the seismic performance of BRKBTMF. The results show BRKBTMF has excellent seismic performance with well controlled structural responses and resistance against collapse. In addition, life cycle repair cost of BRKBTMF was assessed using the next-generation performance-based earthquake engineering framework. The results confirm that BRKBTMF can effectively control the structural and non-structural component damages and minimize the repair costs of the structure under different ranges of earthquake shaking intensities. This studies conclude that BRKBTMF is a viable and effective seismic force resisting system.

KEYWORDS buckling restrained brace, innovative structural system, collapse simulation, seismic assessment

1 Introduction

Buckling restrained knee braced truss moment frame (BRKBTMF) is a novel and innovative steel structural system that utilizes the advantages of long-span trusses and dedicated structural fuses for seismic applications [1–3]. Truss girders are very economical and effective in spanning large distance, however, steel trusses are typically not suitable for seismic application due to its lack of ductility and poor energy dissipation capacity. BRKBTMF utilizes buckling restrained braces (BRBs) as the designated structural fuses to dissipate the sudden surge of earthquake energy, this allows the BRKBTMF to span long distance and yet very efficient in dissipating the seismic loads.

To study the seismic performance of the BRKBTMF, a 4-story prototype building located in Berkeley, California, USA was designed using the performance-based plastic design (PBPD) procedure proposed by Goel and Chao [4]. Nonlinear finite element model of the prototype building was developed using OpenSees [5]. To properly model the force redistribution within the system, when the BRBs fractured, the direct element removal technique developed by Talaat and Mosalam [6] was used to simulate the progressive collapse of the BRKBTMF. The direct element removal method was first proposed to study the progressive collapse of reinforced concrete and unreinforced masonry buildings. The application of this method to steel

Article history: Received Nov 19, 2015; Accepted Jan 14, 2016

building has not been studied before. This paper utilizes the direct element removal method to study the impact of BRB fractures on the overall system performance. The results show the dynamic responses of the building is significantly different with and without implementing the element removal modeling technique.

The seismic performance of the prototype building was analyzed using a bin of 20 ground motions which were amplitude scaled to multiple earthquake shaking intensities. The results show BRKBTMF has excellent seismic performance with well controlled inter-story drift, floor acceleration and excellence resistance against collapse. Lastly, the life cycle repair cost of BRKBTMF was assessed using the next-generation performance-based earthquake engineering framework. The result confirmed that BRKBTMF can effectively control the structural and non-structural component damage and repair costs under different ranges of earthquake shaking intensities. Hence, it is concluded that BRKBTMF is a viable and effective seismic force resisting system.

2 Prototype building and structural design

A prototype 4-story office building located in Berkeley, California, was selected for this study. Figure 1 shows the floor plan and elevation views of prototype building. The prototype building was designed using the performance-based plastic design (PBPD) procedure proposed by Goel and Chao [4] and the design requirement was based on ASCE7 [7]. PBPD uses the energy balanced concept to design the structure to satisfy the force and drift limits at two different earthquake shaking intensities. In this study, the prototype building was designed to have 2.5% and 3.5% maximum inter-story drift ratio under the Design Based Earthquake (DBE) and Maximum Credible Earthquake (MCE), respectively. The calculated base shear of the building based on PBPD was 17.4% of the building weight. The shaking intensities for the DBE and MCE earthquakes were obtained from site specific study [8] which represents the shaking intensities with 10% and 2% probability of exceedance in 50 years.

Unlike the conventional equivalent lateral force-based design procedure, where the structures are designed for the required forces then checked for drift, the PBPD procedure calculates the element sizes to satisfy the forces and drift limits without iterations. More importantly, PBPD takes the plastic mechanism into the design consideration, which leads to controlled failure mechanism during the strong earthquake shaking. Figure 2(a) shows the desired plastic mechanism, of the BRKBTMF. The columns were pin-connected at the base and the trusses were pin-connected to the column. All the inelastic energy was assumed to be dissipated through the axial deformation of the BRBs. Figure 2(b) shows the capacity design concept for the trusses. The trusses were capacity designed to remain elastic under the maximum BRB forces and the expected gravity loads. Figure 2(c) shows the free body diagram of

Table 1 Structural component sizes

floor	BRB strength [kips]	column sizes		truss chord		
		exterior	interior	top/bottom	diagonal	vertical*
4	172	W24×207	W24×229	2MC8×18.7	2MC6×12	L3.5×3.5×5/16
3	259			2MC10×25	2MC6×15.3	L3.5×3.5×5/16
2	312	W24×279	W24×306	2MC10×28.5	2MC6×15.3	L3.5×3.5×5/16
1	339			2MC10×28.5	2MC8×18.7	L3.5×3.5×5/16

* Exterior vertical chords use double angles section of the current size

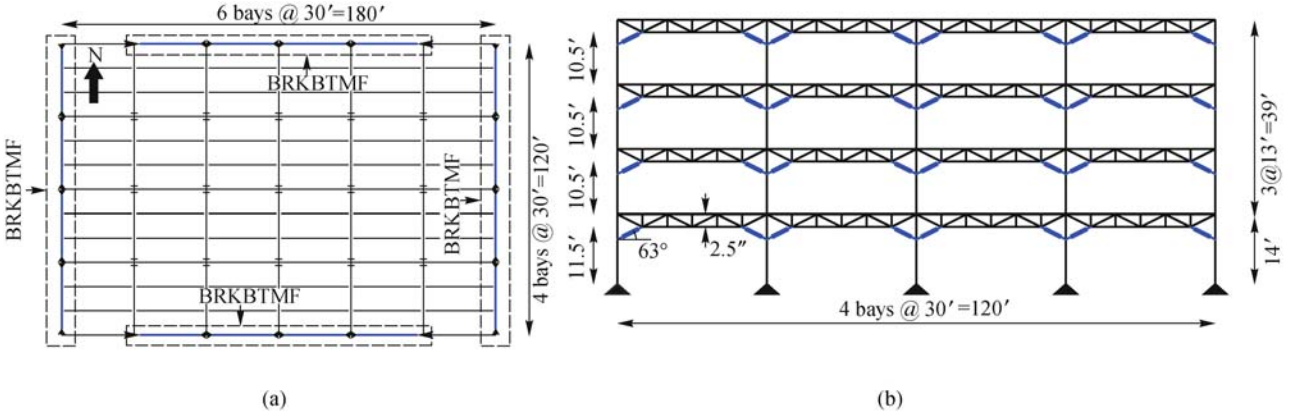

Fig. 1 Prototype building geometry. (a) Floor plan; (b) elevation plan

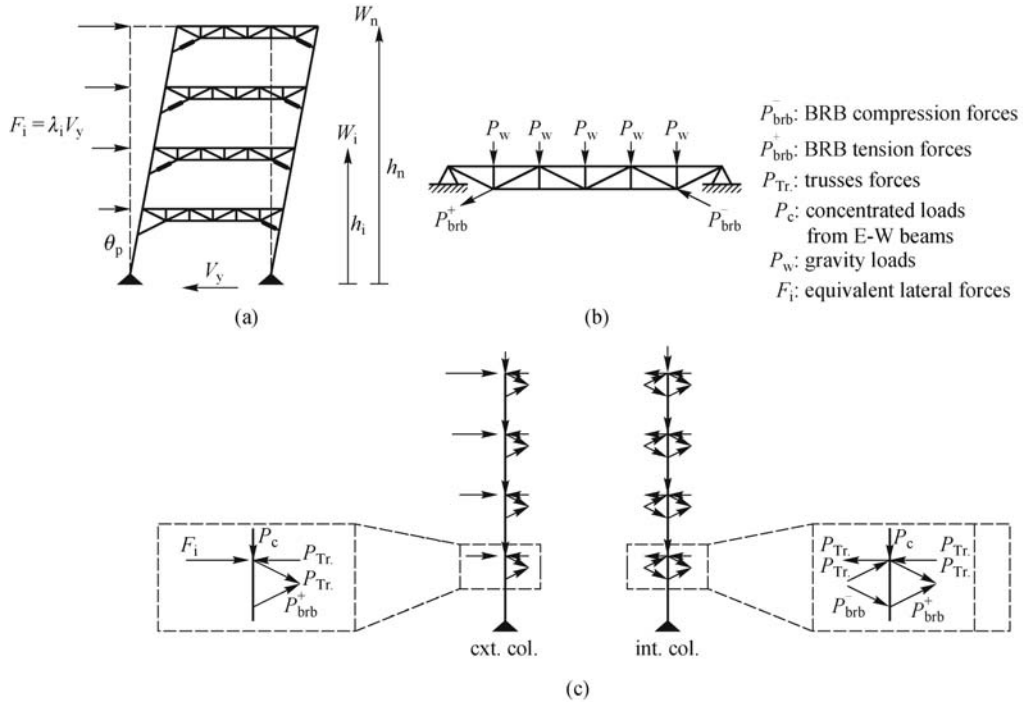

Fig. 2 (a) Plastic mechanism; (b) truss capacity design; (c) column capacity design

the columns. The columns were capacity designed to remain elastic under the maximum expected gravity loads, lateral loads and the BRB forces. Table 1 shows the design sections of the prototype building. Details of the PBPD design procedure for the BRKBTMF can be identified from Wongpakdee et al. [1] and Yang et al. [2,3].

3 Modeling approaches

Nonlinear finite element model of the prototype building was developed using OpenSees [5]. The columns and the trusses were capacity designed to remain elastic, hence they are modeled using elastic beam column elements in OpenSees. The BRBs were modeled using inelastic truss elements with modified Steel02 material. The elastic modulus, yielding strength, strain hardening ratio, and isotropic hardening parameters were calibrated to match the experimental tests conducted by Merritt et al. [9]. The modified Steel02 material was defined to have different tension and compression response calibrated based on the experimental data. Figure 3 shows the calibrated BRB matches the experimental hysteresis. As shown in the experimental tests, the BRB had good energy dissipation capacity. However when BRB axial strain exceeded the strain limit, usually around 2.5%, the BRB will fracture according to tests done by Merritt et al. [9] and summary from López & Sabelli [10]. This is a brittle mode of failure, where the load carrying capacity of the BRB will drop significantly. To properly model the force redistribution

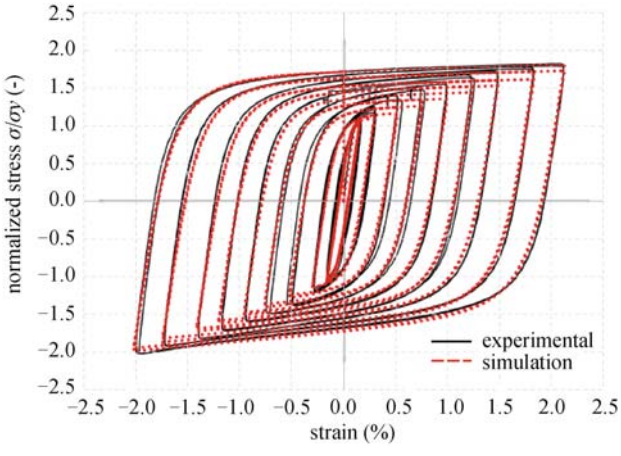

Fig. 3 BRB calibration

within the system, the direct element removal technique developed by Talaat and Mosalam [6] was implemented. The implementation assumed the BRB fracture strain has a lognormal distribution with mean of 2.5% and dispersion of 0.4. In other words, 50% of the BRB will fracture when the BRB reached an axial strain of 2.5%. Figure 4 shows the flow chart for the direct element removal technique implementation. At the beginning of the analysis, a strain demand was checked against the strain capacity, which was calculated using a random number generator with lognormal distribution with mean of 2.5% and dispersion of 0.4. At each stage of the analysis, the BRB strain demand was compared with the strain capacity. If the BRB

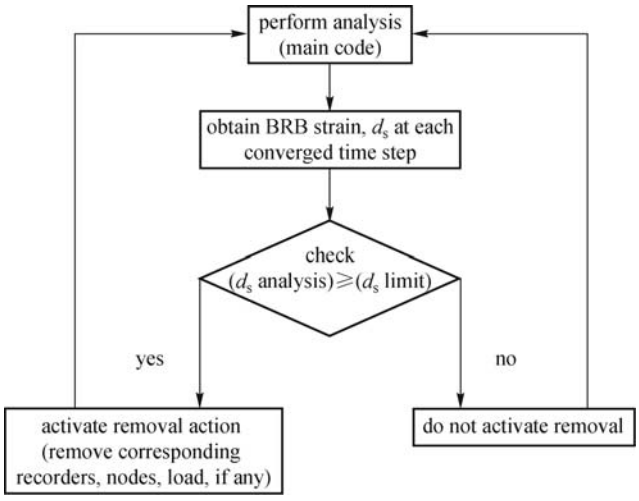

Fig. 4 Element removal procedure

strain was less than the capacity, element removal would not be triggered and the analysis would be carried on as usual. If the BRB strain exceeded the strain capacity, the element removal technique would be triggered and those BRBs would be removed. Similarly, the associated nodes and recorders would be also updated to avoid any computational errors. The stiffness matrix would be updated before next analysis step to allow the model to accurately simulate the force re-distribution within the system. This modeling technique allows the analytical model to systematically simulate the force redistribution within the system, hence able to successfully model progressive collapse of the structure.

4 Comparison of seismic behavior with and without the element removal technique

To compare the system behavior of the building with and without the element removal technique, the 1994 Northridge record was used. The ground motion was scaled to 1/3, 1 and 1.5 times of the MCE hazard to represent three earthquake shaking intensities. The first floor inter-story drift ratios, accelerations, and axial column demands under the three shaking intensities are plotted in Fig. 5.

As shown in Fig. 5, under the 1/3 MCE hazard level, all BRB axial strain demands were within the strain limit.

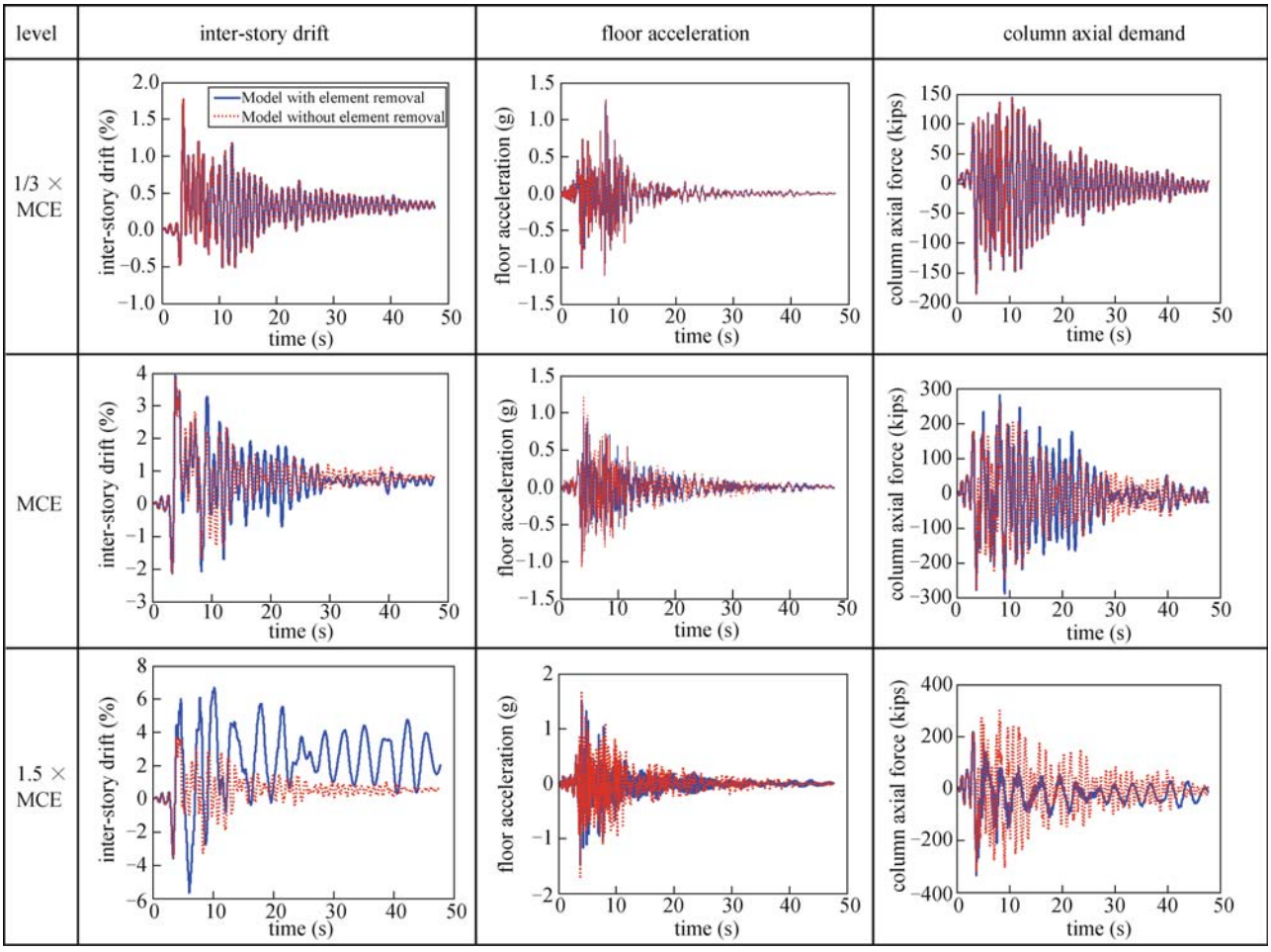

Fig. 5 Seismic behavior comparison on element removal modeling

Table 2 Summary of ground motions

year	event	station	Mw (moment magnitude)	Vs30 (ft./s)	distance to the fault (miles)	scaling factor		
						2/50	10/50	50/50
1976	Friuli, Italy	Tolmezzo	6.50	1394.0	9.8	3.38	1.91	0.69
1976	Gazli, USSR	Karakyr	6.80	2164.0	3.4	2.06	1.16	0.42
1978	Tabas, Iran	Dayhook	7.35	2492.1	8.6	3.70	2.08	0.75
1984	Morgan Hill, US	Coyote Lake Dam	6.19	2615.4	0.3	1.68	0.95	0.34
1984	Morgan Hill, US	Gilroy Array	6.19	2176.2	6.2	3.33	1.87	0.68
1985	Nahanni, Canada	Site 1	6.76	2164.0	6.0	3.01	1.70	0.61
1985	Nahanni, Canada	Site 2	6.76	2164.0	3.0	4.54	2.56	0.92
1989	Loma Prieta, US	BRAN	6.93	1233.9	6.6	1.96	1.11	0.40
1989	Loma Prieta, US	Corralitos	6.93	1516.4	2.4	2.21	1.24	0.45
1989	Loma Prieta, US	Saratoga-Aloha Ave	6.93	1516.4	5.3	4.06	2.29	0.83
1992	Cape Mendocino	Cape Mendocino	7.01	1685.3	4.3	1.67	0.94	0.34
1992	Landers	Lucerne	7.28	2247.0	1.3	4.27	2.40	0.87
1994	Northridge	LA Dam	6.69	2063.6	3.6	3.62	2.04	0.74
1995	Kobe, Japan	Nishi-Akashi	6.90	1998.0	4.4	3.01	1.70	0.61
1994	Northridge, US	Sepulveda VA Hospital	6.69	1247.1	5.2	1.86	1.05	0.38
1994	Northridg, US	LA Dam	6.69	2063.7	3.7	3.62	2.04	0.74
1999	Chi-Chi, Taiwan, China	CHY006	7.62	1437.7	6.1	2.63	1.48	0.53
1976	Friuli, Italy	Tolmezzo	6.5	1393.7	9.8	3.38	1.91	0.69
1999	Chi-Chi, Taiwan, China	TCU078	7.62	1453.4	5.1	3.45	1.94	0.70
1999	Hector Mine, US	Hector	7.13	2247.0	7.3	3.31	1.87	0.67

Hence, the results between two techniques (with and without implementing the element removal technique) were identical. At the MCE hazard level, some BRBs fractured, which resulted to different behaviors between these two modeling techniques. The results show the model with element removal technique experienced larger inter-story drift than the one without element removal. Because the forces were redistributed to other elements after the fractured elements were removal, this resulted to more structural damages. On the other hand, the peak floor acceleration tended to reduce as the system stiffness reduced after the BRB fractured. Similar behavior was observed in the column axial demand, where the demand reduced when the BRB removal technique was implemented. At the 1.5 times MCE hazard level, the maximum difference between these two modeling approaches can be as high as 50%. This shows the importance to implement the element removal technique to quantifying the seismic response of the BRKBTMF.

5 Assessment of the BRKBTMF against collapse

With the element removal technique (as presented in the previous session) implemented, the nonlinear static and dynamic responses of the prototype building were studied. Figure 6 shows the pushover curve for the prototype building. As shown in Fig. 6, the prototype building has a yield base shear of 15% of the weight of the building, which is very close to the design base shear 17% of the weight of the building. Most of the first-story BRBs yielded when the roof top drift ranged between 0.4% and 0.6%. Similarly, the second-, third- and fourth- story BRBs yielded when the roof drift was within 0.5% and 0.75%, 0.6% and 1.1%, 1.0% to 1.5%, respectively. The BRB first fractured when the roof drift reached 2%. The over-strength, Ω, defined as the ratio of the ultimate force divided by the yield force is 1.3. The ductility ratio, μ, defined as the ratio of deformation at 80% of the ultimate strength at the softening range to the yield deformation, is 5. Overall, the BRKBTMF performed well with relatively high stiffness and moderate over-strength factor.

Nonlinear time history analyses were conducted to simulate the behavior of the BRKBTMF. 20 ground motions were selected from the PEER database [11]. The ground motions were amplitude scaled to match the target spectra at three hazard levels: 2%, 10% and 50% probability of exceedance in 50 years. These are denoted as 2/50, 10/50, 50/50, respectively. The hazard analysis was obtained from the UCB seismic guideline (2009) and ground motions were scaled according to ASCE 7 (2010).

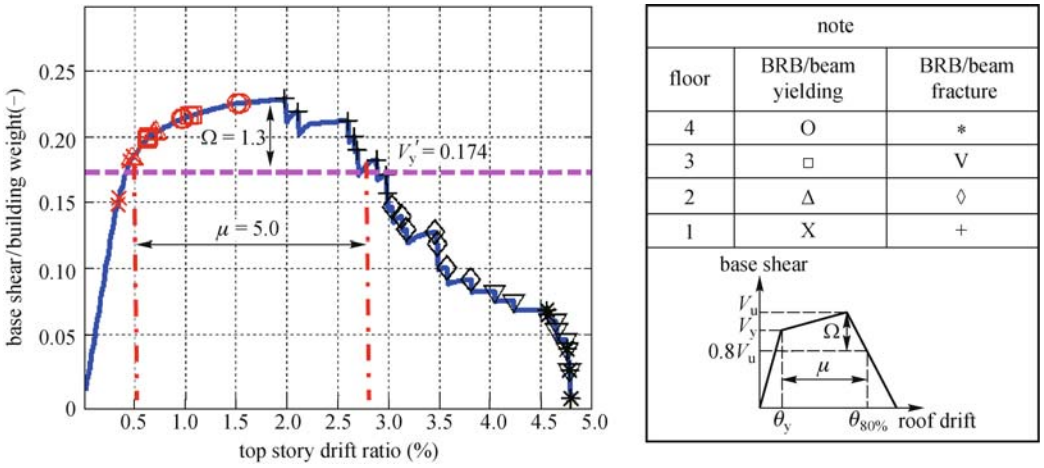

Fig. 6 Pushover analysis

Figure 7(a) shows the target spectra of three hazard levels considered and Fig. 7(b) shows the sample scaled spectra at the 2/50 hazard level. Table 2 shows the summary of all ground motions included in this study. Figure 8 shows the median peak response of the prototype building. The result shows the median peak inter-story drift was less than 2.5%

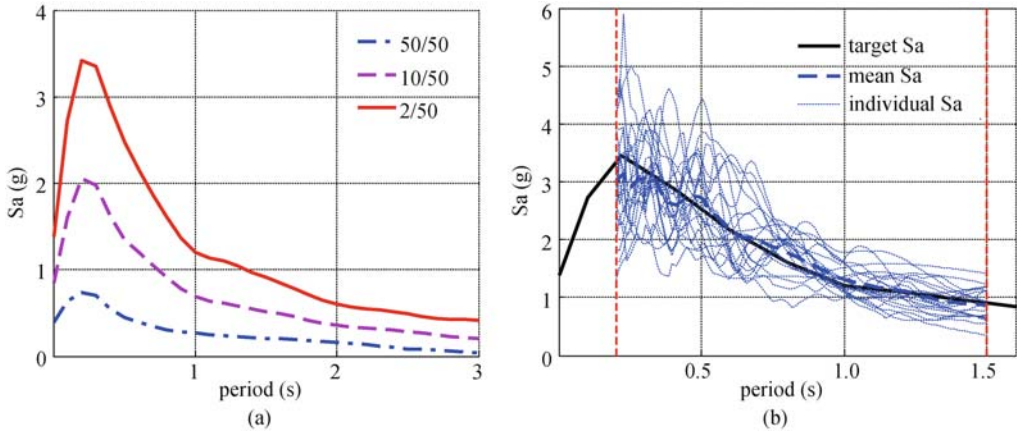

Fig. 7 Ground motion scaling. (a) Target spectrum; (b) ground motion scaling for 2/50 hazard

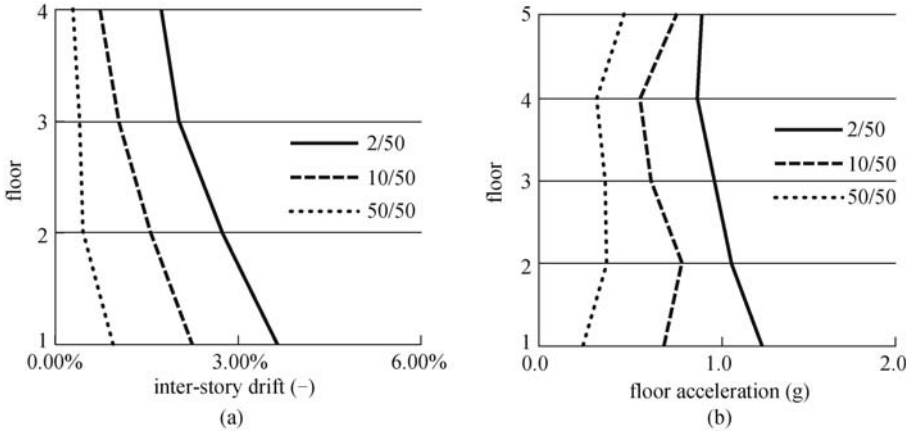

Fig. 8 Peak structural response. (a) peak inter-story drift; (b) peak floor acceleration

and 3.5% for the 10/50 and 2/50 hazard levels, respectively. This confirmed the PBPD approach presented can be used to design the BRKBTMF.

To further assess the seismic safety of the proposed building against collapse. Incremental dynamic analysis (IDA) [12] was conducted to assess the structural collapse margin. Figure 9(a) shows the IDA response of the prototype building. The vertical axis represents the shaking intensity. The horizontal axis represents the maximum inter-story drift ratio. When the IDA curve becomes flat, this means the structure start to become unstable (large increase in deformation with small increase in load), such intensity is defined as the collapse intensity for the structure. Figure 9(b) shows the collapse probability curve obtained from the IDA. It is observed that the probability of collapse at MCE shaking intensity was about 0.1 (Sa_{T1} = 1.18g). The median collapse probability (50% probability of collapse) was about 1.95g. Hence, this shows the structure had a collapse margin ratio (CMR) of 1.65.

6 Life-cycle performance assessment

The life-cycle performance assessment of the BRKBTMF, was analyzed using the next-generation performance-based earthquake engineering (PBEE) assessment framework developed by Yang et al. [13,14] and ATC-58 [15]. The methodology used a Monte Carlo simulation procedure to quantify the seismic performance of the facilities under different earthquake shaking intensities. To expedite the evaluation process, major structural and nonstructural components of the prototype building were identified and grouped into 25 performance groups (PG) as shown in Table 3. PG 1–4 were the structural components; PG 5–8 were the exterior nonstructural components; PG 9–12 and 13–16 were the interior drift- and acceleration- sensitive nonstructural PG; PG 17–20 were the contents; PG 21 was the roof equipment and PG 22–25 were gravity system PG. Each PG consisted of a collection of building components whose performance was similarly affected by a particular engineering demand parameter (EDP). For example, the structural components were assigned to performance groups whose performance was associated with inter-story drift in the story where the components were located. The nonstructural components and contents were sub-divided into displacement-sensitive and acceleration-sensitive groups. The displacement-sensitive groups used inter-story drift ratios to define the performance, while the acceleration-sensitive groups used absolute floor level accelerations. Table 4 shows the sample summary of the quantities and actions required to repair each of the component in the each damage state. The information presented in Tables 3 and 4 are adopted from Yang et al. [13] and from the ATC-58 database [15].

Multiple damage states were defined for each performance group. The damage states were established at points along the damage continuum for which significant repair action would likely be triggered. For each damage state, a damage model (fragility relation) defined the conditional probability of damage being less than or equal to the threshold damage given the value of the engineering demand parameter associated with the performance group. Figure 10 shows the fragility relations used in this study. The horizontal axis represents the EDP, such as peak inter-story drift ratio and floor acceleration experienced by the components. The vertical axis represents the probability of the component in each DSs. For example, Fig. 10(a) shows the fragility curve for the structural PG for the BRKBTMF with 30 ft. span. The BRB is assumed to be either undamaged (DS1) or damaged (DS2). The median and dispersion of the fracture and buckling axial strain was selected as 2.5% and 0.4, respectively. Using the geometry transformation presented in Yang et al. [2], the median inter-story drift ratio which causes the BRB to be damaged can be calculated as 3.1%. Using the peak inter-story drifts

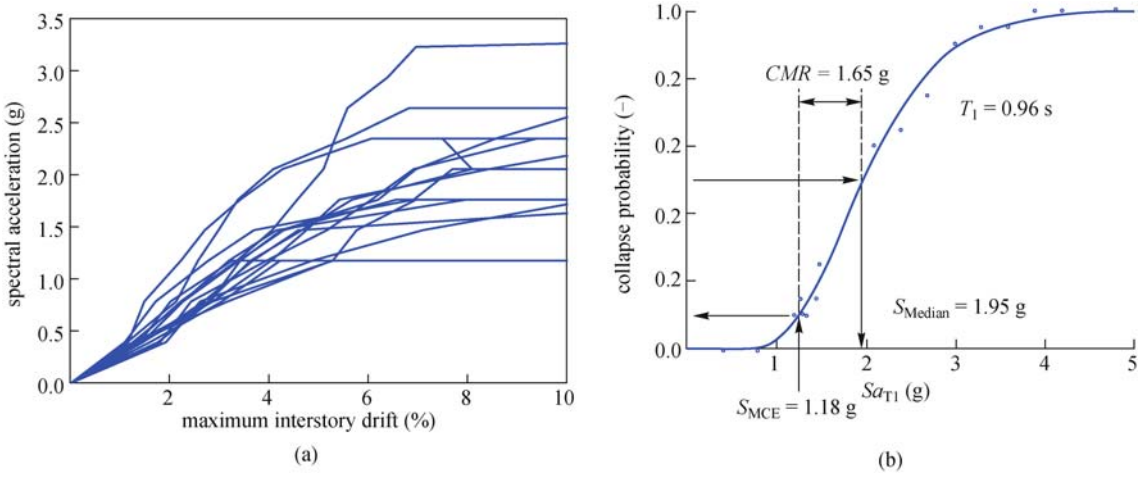

Fig. 9 Incremental dynamic analysis. (a) Dynamic response; (b) building fragility curve

Table 3 Summary of performance groups

PG No.	PG Name	EDP	EDP description	PG description
1	SH12	du_1	inter-story drift between levels 1 and 2	structural: seismic-force-resisting system (displacement sensitive)
2	SH23	du_2	inter-story drift between levels 2 and 3	
3	SH34	du_3	inter-story drift between levels 3 and 4	
4	SH4R	du_4	inter-story drift between levels 4 and roof	
5	EXTD12	du_1	inter-story drift between levels 1 and 2	exterior non-structural (displacement sensitive)
6	EXTD23	du_2	inter-story drift between levels 2 and 3	
7	EXTD34	du_3	inter-story drift between levels 3 and 4	
8	EXTD4R	du_4	inter-story drift between levels 4 and roof	
9	INTD12	du_1	inter-story drift between levels 1 and 2	interior non-structural (displacement sensitive)
10	INTD23	du_2	inter-story drift between levels 2 and 3	
11	INTD34	du_3	inter-story drift between levels 3 and 4	
12	INTD4R	du_4	inter-story drift between levels 3 and roof	
13	INTA2	a_2	total acceleration at level 2	interior non-structural (acceleration sensitive)
14	INTA3	a_3	total acceleration at level 3	
15	INTA4	a_4	total acceleration at level 4	
16	INTAR	a_R	total acceleration at roof	
17	CONT1	a_g	ground acceleration	contents
18	CONT2	a_2	total acceleration at level 2	
19	CONT3	a_3	total acceleration at level 3	
20	CONT4	a_4	total acceleration at level 4	
21	EQUIPR	a_R	total acceleration at roof	rooftop equipment
22	GS12	du_1	inter-story drift between levels 1 and 2	gravity system (displacement sensitive)
23	GS23	du_2	inter-story drift between levels 2 and 3	
24	GS34	du_3	inter-story drift between levels 3 and 4	
25	GS4R	du_4	inter-story drift between levels 4 and roof	

obtained from the nonlinear time history analyses, the probability for each component in each DS can be identified. For example, if the maximum 1st story inter-story drift for the BRKBTMF configuration is 4%, there is a 62% probability that the BRB will fracture and 38% probability that the BRB will be undamaged. Some PGs have more than 2 DSs, such as the one in Fig. 10(g) which have 4 DSs. If the first-story inter-story drift ratio is 5.0%, there is approximately 36% probability that the components in this PG will be in DS1 (undamaged); 54% probability those components will be in DS2 (yielding), 8% in DS3 (partial fracture) and 2% in DS4 (fracture). Using a random number generator between 0 and 1, the DS for each PG could be identified. Once the DS of the component was identified, the repair action, the associate repair cost including labor cost and repair time could be identified from a look up table as shown in Table 4 (ATC58, 2008). The total repair cost for the entire building was then calculated by summing the repair cost from each individual component included in the study. The process is repeated a large number of times to get a distribution of the total repair cost for a range of earthquake intensities. Details of the performance assessment procedure are outlined in Yang et al. [14].

Figures 11(a–c) show the deaggregation of the total repair cost of the prototype building under the 50/50, 10/50, 2/50 hazard levels, respectively. In the 50/50 hazard level, the repair cost is only concentrated in the first story interior nonstructural components (PG 9). As the shaking intensity increases to 10/50 hazard level, structural components (PGs 1–2), nonstructural exterior components (PGs 5–6) and interior nonstructural components (PGs 9–12) and gravity system (PGs 22–25) at the first two floors started to contribute to the repair cost. As the intensity increases to 2/50 hazard level, the structural components and nonstructural exterior components (PGs 1–8), the interior nonstructural components (PGs 9–12) and gravity system (PGs 22–25) also contributed to partial damages. Figure 11(d) shows the cumulative distribution function (CDF) of the total repair cost for the three hazard levels considered. Note that the cost simulation also considered the collapse probability. If the collapse was detected, the building replacement cost was used as the total repair costs. The result showed that the repair cost became higher

Table 4 Sample of repairable component costs for the structure

repair component	unit	repair quantity				unit repair cost			
		DS1	DS2	DS3	DS4	min. quantity	max. cost	max. quantity	min. cost
structural performance group									
BRBs and connections	ea	0	16	——	——	3	$17000	7	$11600
beams – column connections	ea	0	2	24	24	6	$16640	24	$11100
slab replacement	ft^2 *	0	1600	——	——	100	$20	1000	$16
exterior non-structural performance group (displacement sensitive)									
erect scaffolding	ft^2	0	6000	6000	——	1000	$2.5	10000	$2
precast panels removal	ft^2	0	0	8400	——	3000	$12	10000	$8
interior non-structural performance group (displacement sensitive)									
door and frame removal	ea	0	8	8	——	12	$40	48	$25
carpet removal	ft^2	0	0	10000	——	1000	$1.5	20000	$1
interior non-structural performance group (acceleration sensitive)									
furniture removal	ft^2	0	4000	10000	20000	100	$2	1000	$1.25
ceiling system removal	ft^2	0	0	0	20000	1000	$2	20000	$1.25
contents									
papers/books	ft^2	0	0	10000	10000	1000	$0.1	10000	$0.06
office equipment	ft^2	0	5000	10000	10000	1000	$0.06	10000	$0.04
rooftop equipment									
in situ repair		0	1	1	——	1	$10000	2	$10000
remove & replace		0	0	1	——	1	$200000	2	$200000

* 1 ft^2 = 0.09 m^2

as the earthquake intensity increased. The information presented here could be used to make risk management decisions. For example, the prototype building had a median (50% probability of exceedance) repair cost of 35% of building replacement value under 2/50 hazard level. The median repair cost (50% probability of cost exceedance) of the BRKBTMF are 5%, 10%, and 35% of the total building replacement value at the 50/50, 10/50, 2/50 hazard level, respectively. Each hazard had different annual return rate, the loss curves could be combined using the total probability theory. Figure 12 shows the loss curve of the prototype building. The result shows the prototype building had an annual rate of 0.5%, where the total repair cost would exceed $1 million. The area under the annualized loss curve represents the mean annualized loss (MAL) of the prototype building. The prototype building had a mean annualized repair loss of $21100. If one assumed an annual inflation rate of 2.5%, the total life cycle cost of the prototype building after 50 years would be $252 million. The owner can use this information to make informed risk management decision.

7 Conclusions

Buckling restrained knee braced truss moment frame (BRKBTMF) is a novel and innovative steel structural system that utilizes the advantages of long-span trusses and dedicated structural fuses for seismic applications. In this study, a prototype 4-story office building located in Berkeley, CA, USA was designed using the performance-based plastic design approach. The seismic response of the prototype building was analyzed using OpenSees, where robust buckling restrained brace model and element removal technique were developed and implemented. Detailed collapse assessment and life-cycle cost analysis was conducted. The following findings were observed:

1) The model with and without element removal technique yields very different inter-story drift, floor acceleration and structural member forces. Hence, it is crucial to implement the element removal technique to simulate the seismic response of the BRKBTMF.

2) The performance-based plastic design procedure yields good structural design, where the prototype building has controlled drifts, floor acceleration, and collapse margin ratios.

3) The incremental dynamic analysis shows that the BRKBTMF has well reserved collapse margin ratio.

4) The repair cost study shows the BRKBTMF has controlled structural and non-structural repair costs.

These finding confirmed that BRKBTMF is a viable and effective seismic force resisting system.

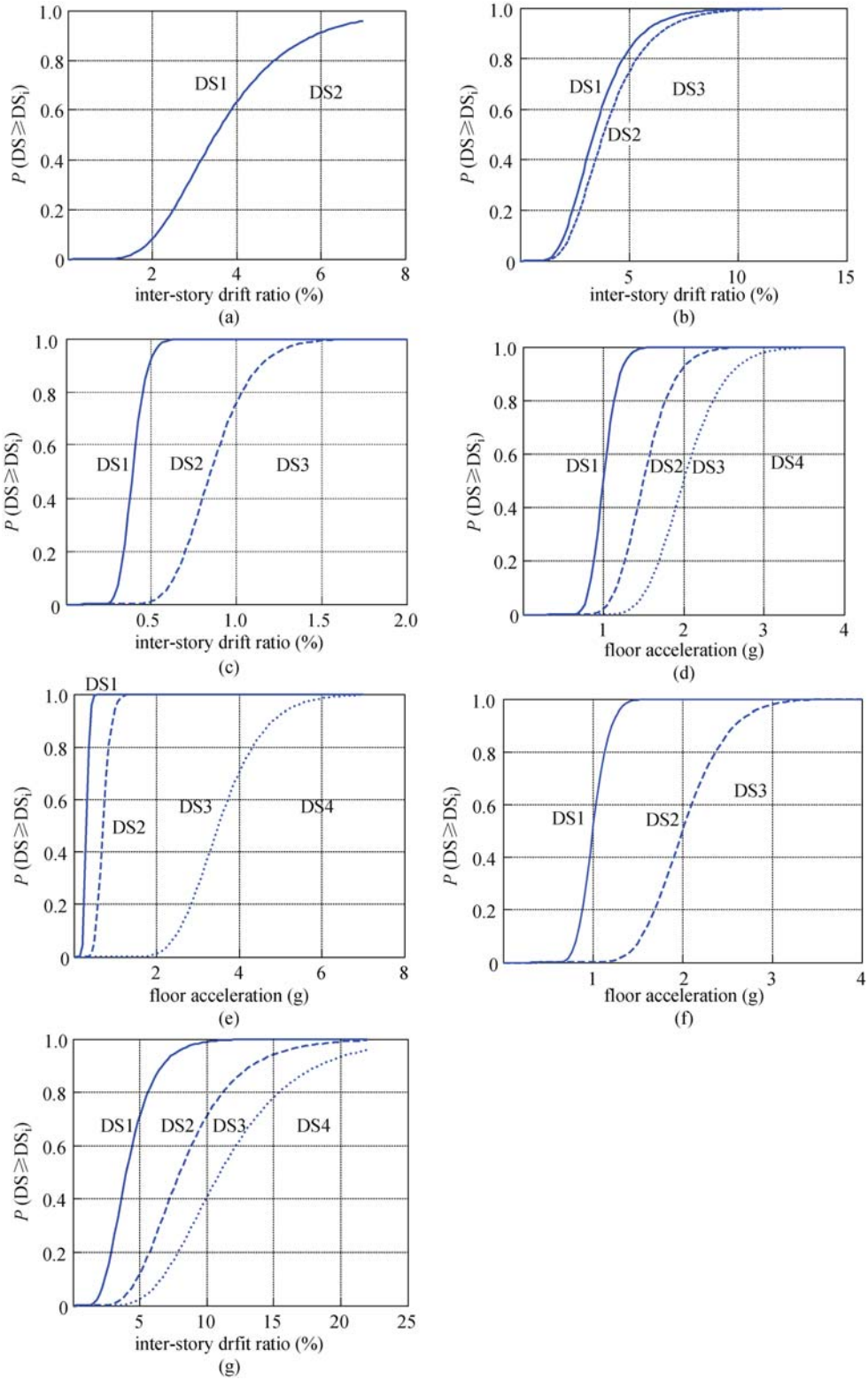

Fig. 10 Fragility curves for performance groups (modified from Yang et al. [13]). (a) Structural PGs (BRB); (b) exterior drift sensitive non-structural PGs; (c) interior drift sensitive non-structural PGs; (d) interior acceleration non-structural PGs; (e) acceleration sensitive contents PGs; (f) roof equipment PGs; (g) gravity system PGs

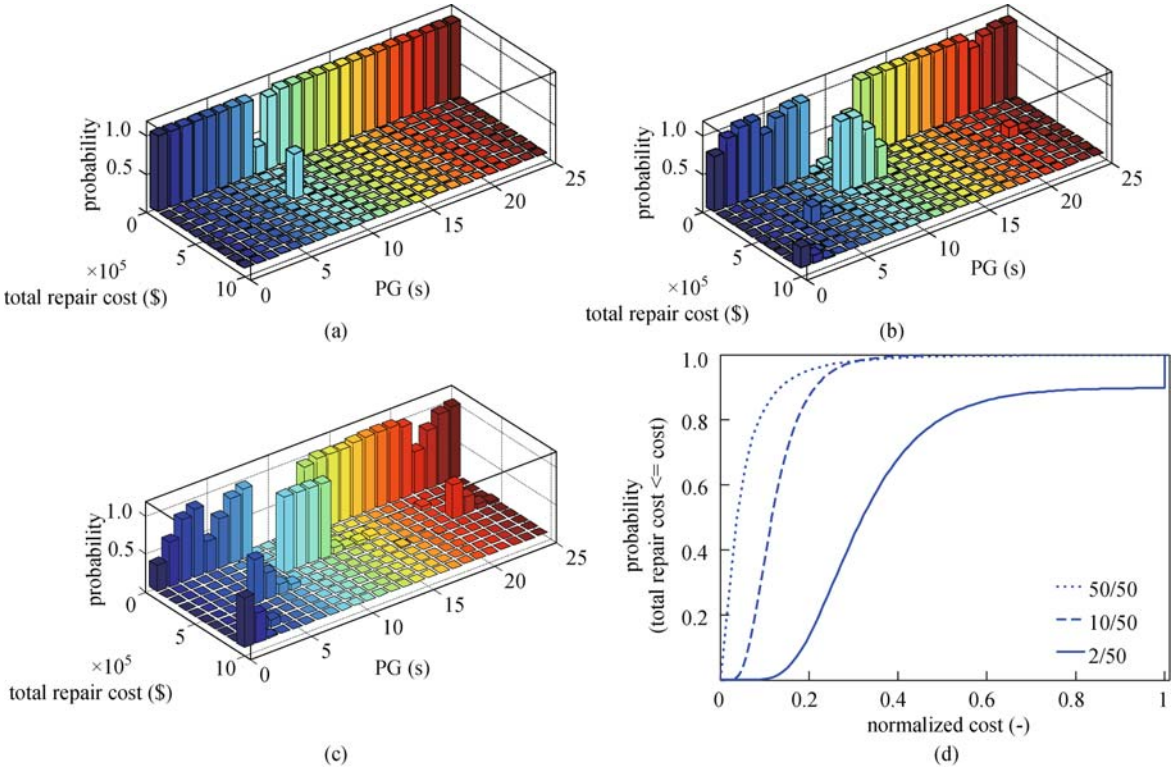

Fig. 11 Repair cost break down under 2% in 50 Yr. hazard. (a) 50/50 hazard level; (b) 10/50 hazard level; (c) 2/50 hazard level; (d) cumulative distributed cost function

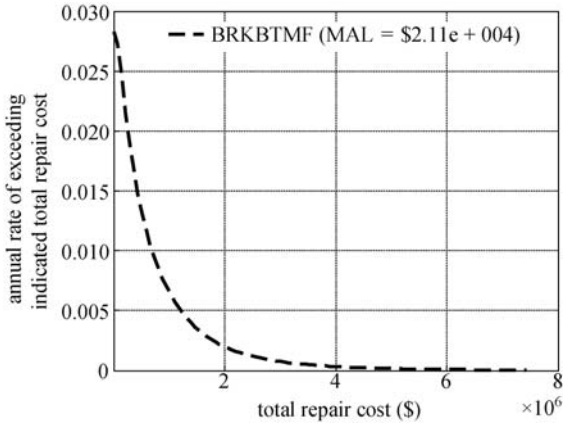

Fig. 12 Life cycle cost for prototype building

Acknowledgements This work was funded in part by the Natural Sciences and Engineering Research Council of Canada (NSERC) jointly with the Steel Structures Education Foundation (SSEF). The authors would like to acknowledge David MacKinnon of the SSEF for making this project possible. The authors would also like to thank: Prof. S. C. Goel form University of Michigan, Prof. S. Leelataviwat from King Mongkut's University of Technology and Mr. John D. Hooper from MKA for their valuable advice during this study. Any opinions, findings and conclusion or recommendations expressed in this material are those of the authors and do not necessarily reflect those of the Natural Sciences and Engineering Research Council of Canada or the Steel Structures Education Foundation.

References

1. Wongpakdee N, Leelataviwat S, Goel S C, Liao W C. Performance-based design and collapse evaluation of buckling restrained knee braced truss moment frames. Engineering Structures, 2014, 60: 23–31
2. Yang T Y, Li Y, Leelataviwat S. Performance-based design and optimization of buckling restrained knee brace truss moment frame. Journal of Performance of Constructed Facilities, 2014, 28(6): A4014007
3. Yang T Y, Li Y, Goel S. Performance evaluation of long-span conventional moment frames and buckling-restrained knee-braced truss moment frames. Journal of Structural Engineering, 2015, 142 (1): 04015081
4. Goel S C, Chao S H. Performance-Based Plastic Design: Earthquake-Resistant Steel Structures. International Code Council, USA, 2008
5. PEER. Open System for Earthquake Engineering Simulation (OpenSees). Pacific Earthquake Engineering Research Center, University of California, Berkeley, CA, 2000
6. Talaat M, Mosalam K M. Modeling progressive collapse in reinforced concrete buildings using direct element removal. Earthquake Engineering & Structural Dynamics, 2009, 38(5): 609–634
7. ASCE. Minimum Design Loads for Buildings and Other Structures. SEI/ASCE 7–10. Reston, VA, USA, 2010
8. UCB. U.C. Berkeley Seismic Guideline. University of California, Berkeley, 2003

9. Merritt S, Uang C M, Benzoni G. Subassemblage Testing of CoreBrace Buckling Resitrained Brace. Report No. TR-2003/01, University of California, San Diego, CA, USA, 2003
10. López W A, Sabelli R. Seismic design of buckling-restrained braced frames. Steel tips, 2004
11. PEER. PEER Strong Motion Database. University of California at Berkeley, 2010 (Retrieved from http://peer.berkeley.edu/peer_ground_motion_database)
12. Vamvatsikos D, Cornell C A. Incremental Dynamic Analysis. Earthquake Engineering & Structural Dynamics, 2002, 31(3): 491–514
13. Yang T Y, Moehle J P, Stojadinovic B. Performance Evaluation of Innovative Steel Braced Frames – PEER Report 2009/103. Pacific Earthquake Engineering Research Center, College of Engineering, University of California, Berkeley, CA, USA, 2009
14. Yang T Y, Moehle J P, Stojadinovic B, Der Kiureghian A. Seismic performance evaluation of facilities: Methodology and implementation. Journal of Structural Engineering, 2009, 135(10): 1146–1154
15. Applied Technology Council. Development of next-generation performance-based seismic design procedures for new and existing buildings, 2012 (https://www.atcouncil.org/projects-sp-1235934887/project-atc58)